Cell

The Histone Variant H2A.W Defines Heterochromatin and Promotes Chromatin Condensation in *Arabidopsis*

Ramesh Yelagandula,[1,2,8] Hume Stroud,[3,8,10] Sarah Holec,[1] Keda Zhou,[6] Suhua Feng,[3,4,5] Xuehua Zhong,[3,9] Uma M. Muthurajan,[6] Xin Nie,[1,2] Tomokazu Kawashima,[1] Martin Groth,[3,5] Karolin Luger,[6,7] Steven E. Jacobsen,[3,4,5,*] and Frédéric Berger[1,2,*]

[1]Temasek Lifesciences Laboratory, 1 Research Link, National University of Singapore, 117604 Singapore, Singapore
[2]Department of Biological Sciences, National University of Singapore, 14 Science Drive 4, 117543 Singapore, Singapore
[3]Department of Molecular, Cell, and Developmental Biology, University of California, Los Angeles, Los Angeles, CA 90095, USA
[4]Eli and Edythe Broad Center of Regenerative Medicine and Stem Cell Research, University of California, Los Angeles, Los Angeles, CA 90095, USA
[5]Howard Hughes Medical Institute, University of California, Los Angeles, Los Angeles, CA 90095, USA
[6]Department of Biochemistry and Molecular Biology, Colorado State University, Fort Collins, CO 80523, USA
[7]Howard Hughes Medical Institute, Colorado State University, Fort Collins, CO 80523, USA
[8]Co-first author
[9]Present address: Wisconsin Institute for Discovery, Laboratory of Genetics, University of Wisconsin, Madison, WI 53706, USA
[10]Present address: Department of Neurobiology, Harvard Medical School, Boston, MA 02115, USA
*Correspondence: jacobsen@ucla.edu (S.E.J.), fred@tll.org.sg (F.B.)
http://dx.doi.org/10.1016/j.cell.2014.06.006

SUMMARY

Histone variants play crucial roles in gene expression, genome integrity, and chromosome segregation. We report that the four H2A variants in *Arabidopsis* define different genomic features, contributing to overall genomic organization. The histone variant H2A.W marks heterochromatin specifically and acts in synergy with heterochromatic marks H3K9me2 and DNA methylation to maintain transposon silencing. In vitro, H2A.W enhances chromatin condensation by promoting fiber-to-fiber interactions via its conserved C-terminal motif. In vivo, H2A.W is required for heterochromatin condensation, demonstrating that H2A.W plays critical roles in heterochromatin organization. Similarities in conserved motifs between H2A.W and another H2A variant in metazoans suggest that plants and animals share common mechanisms for heterochromatin condensation.

INTRODUCTION

All eukaryotic genomes are packaged into chromatin by nucleosomes, which consist of 146 base pairs of DNA wrapped around an octamer of histones H2A, H2B, H3, and H4 (Luger et al., 1997). Chromatin is organized into transcriptionally active euchromatin and more compact inactive heterochromatin. In somatic cells of *Arabidopsis*, heterochromatin can be visualized as dense structures called chromocenters by DAPI staining (Lysak et al., 2006). In *Schizosaccharomyces pombe* and mammals, heterochromatin is demarcated by histone H3 lysine 9 methylation (H3K9me3) (Jenuwein and Allis, 2001). Similarly, in *Arabidopsis*, heterochromatin is marked by H3K9me2, which is deposited by the histone methyltransferases KRYPTONITE (KYP) and SUVH5 and 6 (Bernatavichute et al., 2008; Jackson et al., 2002; Malagnac et al., 2002). DNA methylation plays an important function in regulating heterochromatin (Law and Jacobsen, 2010). The plant-specific DNA methyltransferase CHROMOMETHYLASE 3 (CMT3) binds to H3K9me2 and methylates cytosine residues at CHG sites (where H is A or C or T) (Du et al., 2012; Lindroth et al., 2001). In addition, DNA methylation in CG contexts is carried out by METHYLTRANSFERASE 1 (MET1) (Finnegan and Dennis, 1993; Law and Jacobsen, 2010). DOMAINS REARRANGED METHYLTRANSFERASE 2 (DRM2) and the recently discovered CHROMOMETHYLASE 2 (CMT2) perform methylation in CHH contexts (Haag and Pikaard, 2011; Zemach et al., 2013; Stroud et al., 2014). DNA methylation and H3K9me2 act together to silence genes and transposable elements (TEs) in *Arabidopsis* (Law and Jacobsen, 2010).

Histone variants carry out diverse chromatin functions, including transcription, DNA repair, and chromosome segregation (Bönisch and Hake, 2012; Millar, 2013; Szenker et al., 2011; Talbert and Henikoff, 2010). The vast majority of known histone variants are homologs of H2A and H3 histones. A phylogenetic analysis of histone families supports the notion that genes encoding ancestral histone H3.3 and H2A.Z duplicated and evolved to encode histone variants with distinct properties (Talbert et al., 2012). In the case of H3, the cell-cycle-controlled H3.1 class evolved independently in most phyla, acquiring similar properties in plants and animals (Filipescu et al., 2013; Stroud et al., 2012; Wollmann et al., 2012). Similarly, the canonical H2A, thereafter referred to simply as "H2A," as well as H2A.X, evolved independently from the ancestral H2A.Z in

almost all eukaryotes (Talbert et al., 2012). In all eukaryotes, the centromeric H3 variant (cenH3) is functionally conserved, specifically recruited at the centromere, and instrumental for kinetochore function (De Rop et al., 2012; Talbert et al., 2008).

Genome-wide profiling of histone variants using chromatin immunoprecipitation followed by deep sequencing (ChIP-seq) revealed that some histone variants decorate specific functional regions of the genome (Talbert and Henikoff, 2010). In yeast and animals, H2A.Z is enriched at transcriptional start sites (TSS) or 5′ ends of genes (Guillemette et al., 2005; Li et al., 2005; Raisner et al., 2005). On the other hand, H3.3 is enriched over gene bodies with inclination toward the 3′ end of genes in *Drosophila* and humans (Goldberg et al., 2010; Mito et al., 2005). Histone variants also colocalize with posttranslational modifications on their own N-terminal tails. For example, H3.3 tends to be associated with H3K4me2/3, whereas H3.1 tends to be enriched at heterochromatin marked by H3K9me2 (Loyola and Almouzni, 2007). Although H2A.Z and H3.3 are predominantly linked to transcriptional activation, they are also associated with heterochromatin maintenance. In yeast, H2A.Z is enriched in subtelomeric regions and prevents spreading of telomeric heterochromatin into euchromatic regions (Meneghini et al., 2003). Similarly, in humans, H3.3 is localized to telomeric heterochromatic regions (Goldberg et al., 2010; Wong et al., 2009). In contrast, in *Arabidopsis*, H2A.Z and H3.3 are excluded from heterochromatin. H2A.Z is enriched at the TSS of expressed genes and also enriched in gene bodies of response genes, which are differentially activated during development or stress (Aceituno et al., 2008; Coleman-Derr and Zilberman, 2012; Zilberman et al., 2008). Similarly, H3.3 enrichment is confined toward the 3′ end of genes and is correlated positively with gene expression (Stroud et al., 2012; Wollmann et al., 2012). Hence, histone variants H2A.Z and H3.3 appear to exclusively define euchromatin in *Arabidopsis*. This observation led us to question whether a specific combination of histone variants defines heterochromatin in plants, and if so, what their impact might be on chromatin organization.

To understand the roles of histone H2A variants in chromatin regulation in *Arabidopsis*, we generated a comprehensive localization map of all four types of H2A variants and found that they demarcate different features of the genome. Interestingly, heterochromatin was specifically marked by the previously uncharacterized H2A variant H2A.W. We find that heterochromatin-specific localization of H2A.W does not depend on H3K9me2 or DNA methylation and that H2A.W and DNA methylation cooperatively silence TEs through independent pathways. In vitro nucleosome array experiments suggest that H2A.W causes higher-order chromatin condensation by promoting chromatin fiber-to-fiber interactions. Finally, our findings further demonstrate that H2A.W is both necessary and sufficient for heterochromatin condensation in vivo.

RESULTS

Genome-wide Profiling of H2A Variants Identifies the Heterochromatin-Specific H2A.W

The *Arabidopsis* genome comprises 13 genes encoding histone H2A variants, which are grouped into four classes according to C-terminal conserved motifs (Figure S1A available online) (Talbert et al., 2012). We obtained antibodies specific and representative of each H2A variant class (Figure S1B). We performed genome-wide profiling by chromatin immunoprecipitation for H2A variant-bound DNA followed by deep sequencing (ChIP-seq) (Figures 1 and S1C). H2A.X covered the entire genome (Figures 1A and S1C). H2A showed a relative depletion at pericentromeric chromatin, as well as over TEs and islands of H3K9me2 present in chromosome arms outside pericentromeric heterochromatin (Figures 1A, 1C, 1D, 1E, and S1C). Both H2A.X and H2A were enriched over gene bodies (Figure 1B). In contrast with the rather uniform profiles of H2A and H2A.X over gene bodies, H2A.Z was enriched specifically at the 5′ end of genes (Figure 1B) and was highly depleted over all heterochromatic features (Figures 1C and 1D), as reported previously (Coleman-Derr and Zilberman, 2012). In addition, we analyzed whether enrichment of each H2A variant over gene bodies depends on the level of gene expression. Comparing quintiles of genes defined by their expression level, we observed gradual depletion of H2A and H2A.X and, in turn, enrichment of H2A.Z when expression levels decreased (Figure 1F). Hence, highly expressed genes are defined by a marked enrichment in H2A.Z and H2A at the 5′ end and 3′ end, respectively, whereas inactive genes are covered by H2A.Z.

Unlike all other H2A variants, H2A.W was strongly depleted from gene bodies (Figure 1B). H2A.W was specifically enriched in pericentromeric heterochromatin, TEs, and islands of H3K9me2 (Figures 1A, 1C–1E, and S1C). The Pearson correlation between H3K9me2 and H2A.W within TEs across the genome was 0.7, indicating a very high degree of overlap between H2A.W and H3K9me2. Overall, we conclude that antagonistic localizations of H2A.Z and H2A.W distinguish active and inactive domains of chromatin.

H2A.W Indexes Heterochromatin

H2A.W carries an extended C-terminal tail with a conserved SPKK (in general T/SPXK) motif (Figure S1A) (Bönisch and Hake, 2012). The H2A.W variant class evolved and is highly conserved in seed-bearing plants (i.e., gymnosperms and angiosperms) (Figure S2A). In *Arabidopsis*, the H2A.W family comprises three proteins—H2A.W.6, H2A.W.7, and H2A.W.12—which are encoded by the genes *HTA6*, *HTA7*, and *HTA12*, respectively (Figure S1A). *HTA6* is expressed at higher levels than the other two H2A.W homologs (Figure S2D) and was used for the ChIP-seq analyses described above. In order to investigate whether the properties of H2A.W.6 revealed by ChIP-seq analysis were representative of the entire H2A.W class, we analyzed the localization of each member of the H2A.W family in vivo. We fused the RED FLUORESCENT PROTEIN (RFP) to each gene encoding H2A.W and expressed the fusion protein under the control of its respective promoter in transgenic plants that were also expressing the CENTROMERIC HISTONE 3 (CenH3) fused to the GFP. CenH3 is located at the centromere of each chromosome and is surrounded by pericentromeric chromatin that forms heterochromatin domains called chromocenters (Fang and Spector, 2005; Talbert et al., 2002; Fransz et al., 2002). Each H2A.W-RFP localized primarily to domains corresponding to the ten chromocenters, each containing a CENH3-GFP patch in its center (Figures

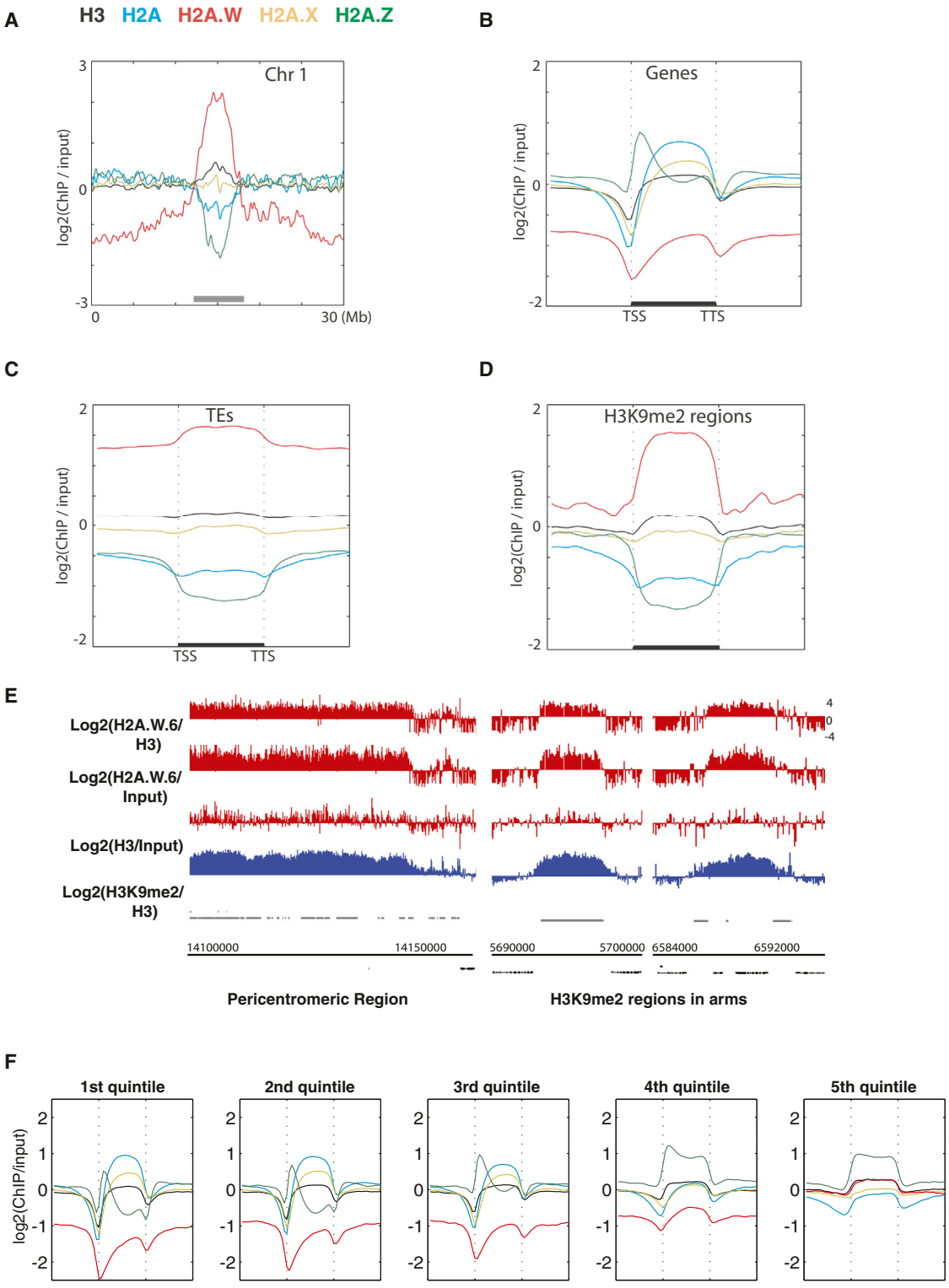

Figure 1. The Histone Variant H2A.W Is Specifically Localized to Heterochromatin

(A) Distribution of ChIP-seq reads along chromosome 1 for each class of H2A variants and total H3, relative to input DNA. The gray bar at the bottom indicates pericentromeric heterochromatin.

(B) Average enrichment of each class of H2A variants and total H3 over genes delimited by a TSS and a transcription termination site (TTS).

(C) Average enrichment of each class of H2A variants and total H3 over TEs.

(legend continued on next page)

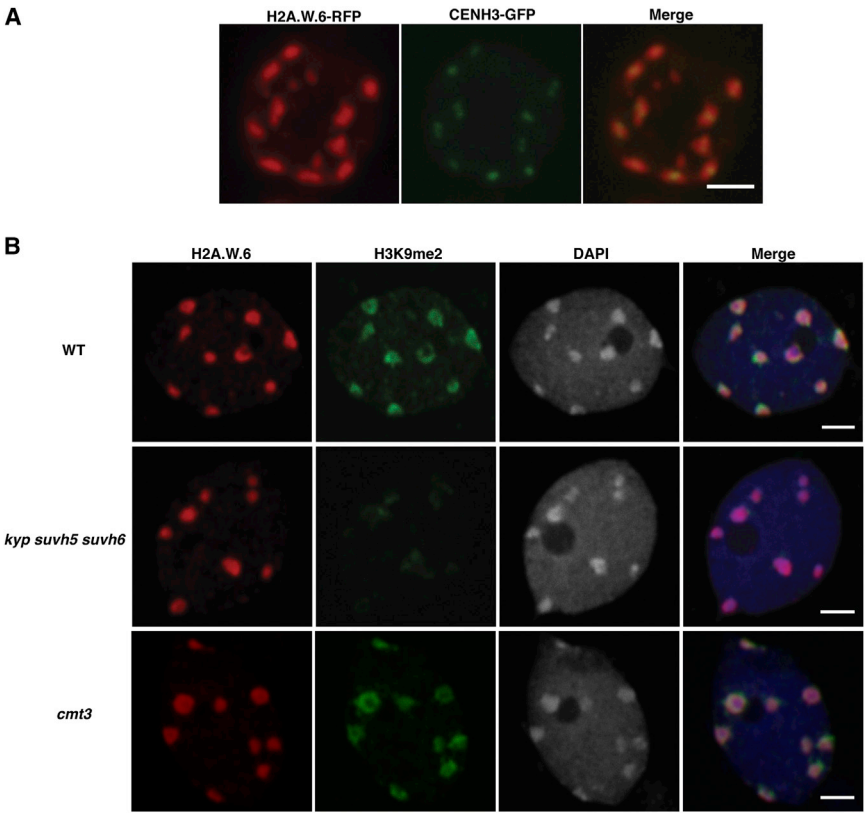

Figure 2. Localization of H2A.W Does Not Depend on H3K9me2 and DNA Methylation

(A) Localization of H2A.W.6 with the centromeric histone CENH3. In vivo confocal section of a root nucleus of transgenic plants expressing p*CENH3::CENH3-GFP* and *pH2A.W.6::H2A.W.6-RFP*.

(B) Confocal sections of leaf nuclei immunostained for H3K9me2 and H2A.W.6 with DAPI counterstaining in genetic backgrounds WT, *kyp suvh5 suvh6*, and *cmt3*. Scale bars represent 2 μm.

See also Figure S2.

2A, S2B, and S2C). H2A.W.7-RFP and H2A.W.12-RFP also colocalized with H3K9me2 (Figures S2E and S2F), as demonstrated for H2A.W.6 (Figure 2B, wild-type [WT] row, and 1D). In conclusion, all members of the H2A.W family are tightly associated with heterochromatin in somatic cells.

Recruitment of H2A.W Is Independent of H3K9me2 or DNA Methylation

The colocalization between H2A.W and H3K9me2 suggested a possible mechanistic link between the deposition of these two heterochromatic features. Preventing H3K9me2 deposition by mutating the three methyltransferases, KYP, SUVH5, and SUVH6, did not significantly alter the pattern of H2A.W.6 (Figure 2B). Similarly, H2A.W.6 localization was not perturbed significantly by the absence of CMT3, the factor that methylates cytosine residues in CHG contexts at heterochromatic loci marked by H3K9me2 (Figure 2B). Because H2A.W localization does not depend on H3K9me2 or the associated CHG methylation, we tested the influence of other pathways responsible for DNA methylation. The loss of the de novo DNA methyltransferase DRM2 did not affect H2A.W or heterochromatin organization (Figures S2G–S2I). In contrast, heterochromatin was partially dispersed in the absence of the CG methyltransferase MET1 or the chromatin remodeling protein DECREASED DNA METHYLATION 1 (DDM1) that contribute to maintenance of DNA methylation and silencing of heterochromatic loci (Figures S2G–S2I) (Vongs et al., 1993; Jeddeloh et al., 1999; Zemach et al., 2013). However, in spite of the change of heterochromatin condensation in *met1* and *ddm1* genetic backgrounds, H2A.W.6 was still colocalized with dispersed heterochromatin marked with H3K9me2 (Figures S2G–S2I). These results suggest that the recruitment or maintenance of H2A.W to heterochromatin depend neither on DNA methylation nor on H3K9me2 and that a mechanism independent from these markers of heterochromatin is responsible for H2A.W deposition. However, other unknown components of heterochromatin might participate in H2A.W localization.

Loss of H2A.W Causes Heterochromatin Decondensation

To study the function of H2A.W in vivo, we obtained knockout lines for all three genes encoding H2A.W (Figure S3A). In single mutants, we did not observe any obvious visible phenotype. Significant growth defects were observed in *h2a.w.6 h2a.w.7* and *h2a.w.6 h2a.w.12* double mutants, and plant growth was severely affected in *h2a.w.6 h2a.w.7 h2a.w.12* (*h2a.w*) triple mutants (Figure 3A and data not shown). The strong effect of

(D) Average enrichment of each class of H2A variants and total H3 over defined H3K9me2 enriched regions in chromosomal arms. In (B)–(D), the middle region marked by the horizontal black bar represents the body of the element considered. The left and right flanking regions represent the 5′ upstream and the 3′ downstream regions, respectively.

(E) Genome browser views of H2A.W.6 enrichment over pericentromeric chromatin and over a H3K9me2 enriched region in the arm of a chromosome. Black bars represent genes, and gray bars represent TEs. The log2 ratios of H2A.W to input genomic DNA and H2A.W to total H3 are shown.

(F) Average enrichment of each class of H2A variants and total H3 over genes as defined in (B). Genes were grouped in quintiles defining highest (first quintile) to lowest (fifth quintile) transcription levels in 10-day-old seedlings.

See also Figure S1.

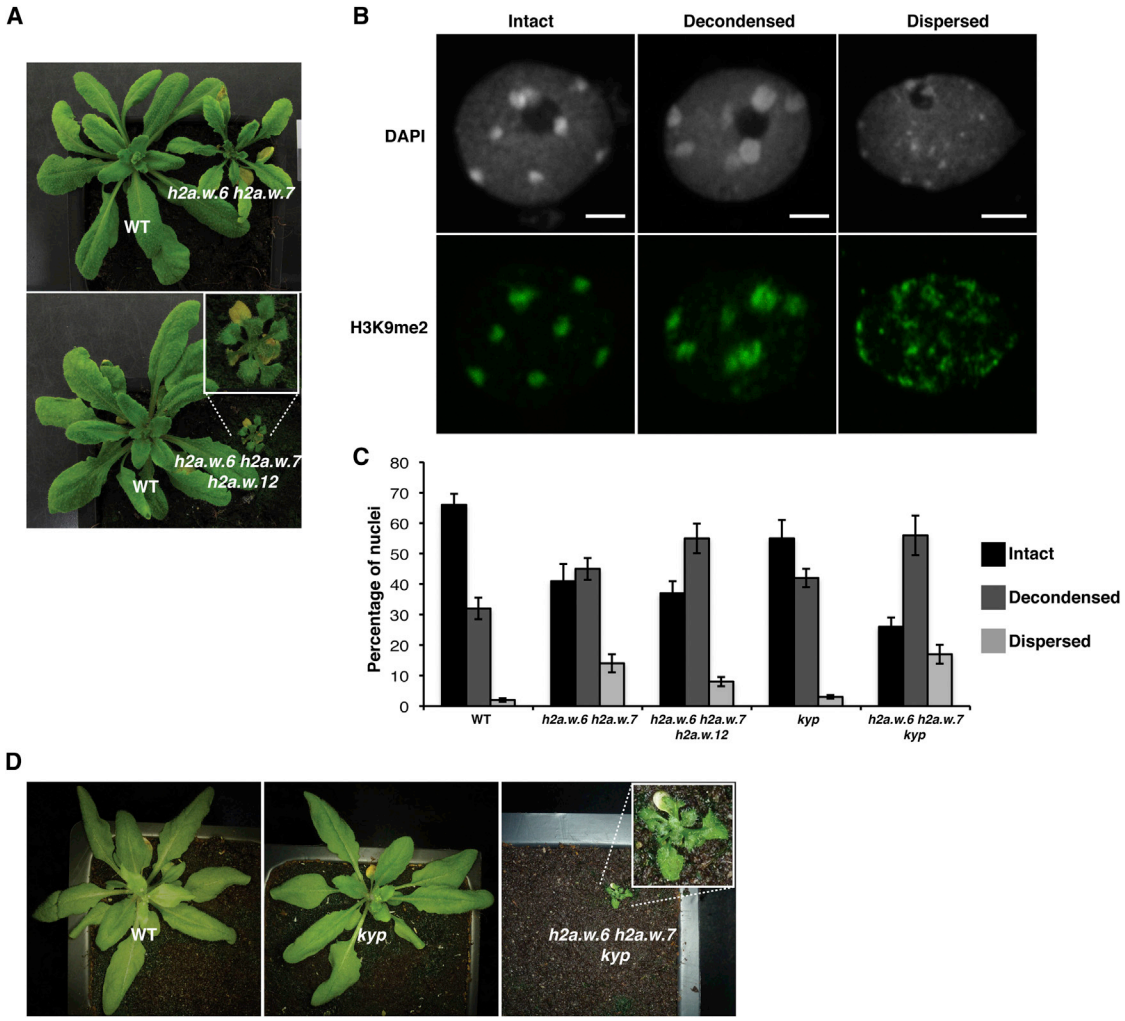

Figure 3. H2A.W Is Required for Heterochromatin Condensation

(A) Morphological phenotypes observed in *h2a.w* double and triple mutants growing side by side with WT plants. The triple mutant shown in the main panel is magnified in the inset.

(B) Decondensed chromocenters observed in leaf nuclei stained with DAPI and immunostained against the heterochromatin marker H3K9me2. Scale bars represent 2 μm.

(C) The bar chart represents percentages of nuclei belonging to each class of nuclei shown in (B) based on the degree of decondensation of chromocenters observed in DAPI staining. Error bars represent SD.

(D) Morphological phenotype observed in the *h2a.w.6 h2a.w.7 kyp* mutant growing side by side with a WT plant. The triple mutant shown in the main panel is magnified in the inset.

See also Figure S3.

h2a.w.6 is likely due to its high level of expression among the three H2A.W encoding genes (Figure S2D). Triple mutant plants failed to flower and did not give rise to the next generation, suggesting that H2A.W is essential. Because H2A.W is specifically localized to heterochromatin, we analyzed heterochromatin structure in nuclei of *h2a.w* knockout plants. In the double and triple mutants, a significant proportion of nuclei showed variable degrees of physical expansion of heterochromatin marked by H3K9me2 (Figure 3B), reaching in some nuclei a dispersed state in which chromocenters were no longer defined by condensed DAPI staining (Figure 3C). We conclude that H2A.W is required for heterochromatin condensation.

Because heterochromatin was disorganized in *h2a.w* mutant, we analyzed the localization of the conserved heterochromatic mark H3K9me2 in *h2a.w* triple mutants. In this genetic background, H3K9me2 was still localized to DAPI-rich regions even in nuclei with dispersed heterochromatic chromocenters, indicating that H3K9me2 deposition does not require H2A.W (Figure S3B). The independent colocalization of H2A.W and H3K9me2 prompted us to examine the genetic interaction between these two marks of heterochromatin. In the H3K9 methyltransferase mutant *kyp* (Figure S3C), H3K9me2 is reduced but does not show a significant effect on plant growth (Jackson et al., 2002), as SUVH5 and 6 also contribute to H3K9me2

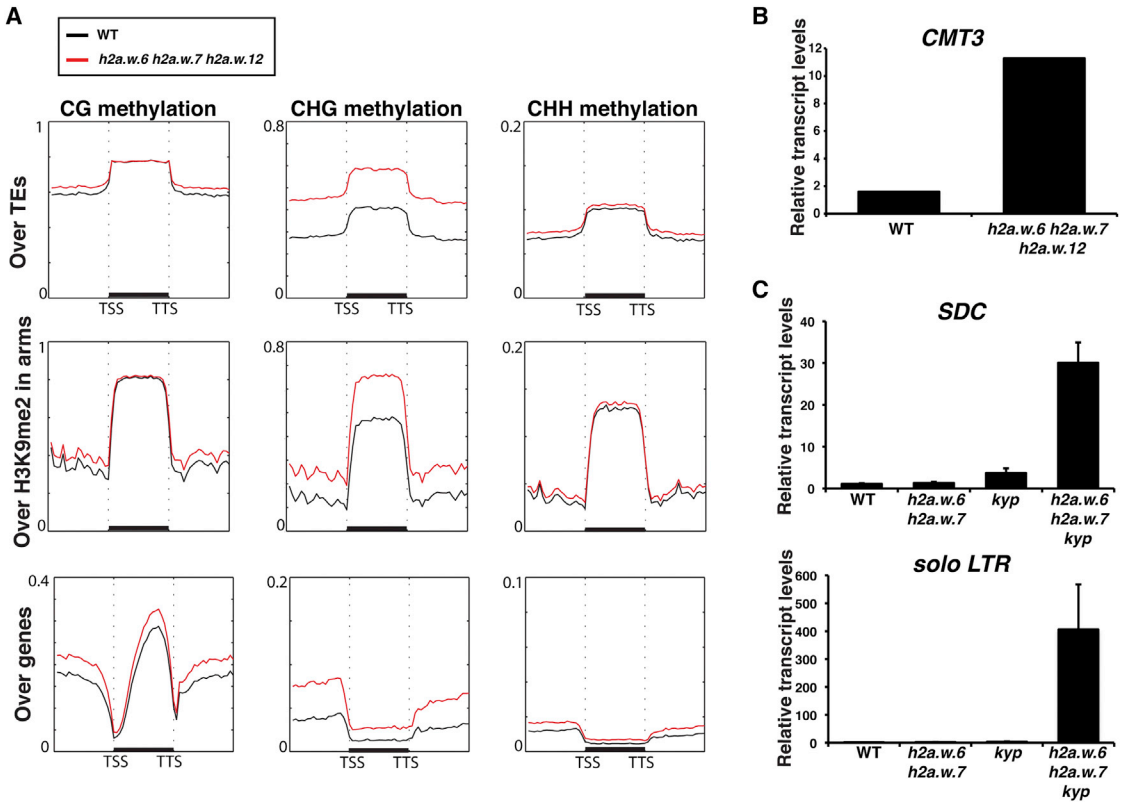

Figure 4. H2A.W Represses the Transcription of Heterochromatic Elements in Synergy with DNA Methylation Mediated by CMT3

(A) Metaplot analysis from whole-genome bisulfite sequencing showing different types of methylation levels in WT and *h2a.w* triple mutant over major genomic features. Graphs were plotted as in Figure 1A.

(B) Expression levels of *CMT3* in *h2a.w* triple mutant in comparison to WT. Expression values were obtained from RNA-seq data.

(C) Expression levels of *SDC* and *solo LTR* in *h2a.w.6 h2a.w.7 kyp* mutant compared with WT. The data from quantitative real-time RT-PCR were normalized to *ACTIN7*. Error bars represent SD based on three independent biological replicates.

See also Figure S4.

(Bernatavichute et al., 2008; Malagnac et al., 2002). We found that simultaneous mutation of KYP and H2A.W in *h2a.w.6, h2a.w.7, kyp* plants caused severe growth defects compared to growth defects observed in *h2a.w.6, h2a.w.7* mutant plants (Figure 3D). Similarly, we also observed an increase in the proportion of nuclei with decondensed heterochromatin (Figure 3C). These results indicate that H2A.W and KYP participate in parallel pathways controlling heterochromatin condensation.

H2A.W Represses Transposable Elements in Synergy with CMT3-Mediated CHG Methylation

Decondensation of heterochromatin in mutants such as *met1* has been previously shown to be associated with increased transcription of TEs and genes in the proximity of heterochromatic loci (Vaillant et al., 2008; Reinders et al., 2009; Law and Jacobsen, 2010). However, RNA sequencing (RNA-seq) analyses of the *h2a.w* triple mutant did not show a substantial impact on expression of TEs (Figure S4A). This suggests that, in the absence of H2A.W, other silencing pathways might play compensatory roles in maintaining the transcriptional repressive status of TEs. Indeed, DNA methylation analysis by whole-genome bisulfite sequencing (BS-seq) in the *h2a.w* triple mutant showed a significant increase in CHG methylation over TEs and regions enriched in H3K9me2, whereas DNA methylation over gene bodies was not affected (Figure 4A). A notable upregulation of the expression of *CMT3* encoding the primary CHG DNA methyltransferase likely accounts for the increase in CHG methylation (Figure 4B). DNA methylation at CG and CHH sites was not significantly affected, suggesting a specific association of H2A.W with CHG methylation (Figure 4A). These results suggested the possibility that increased CHG methylation may compensate for the lack of H2A.W, resulting in maintenance of the transcriptional repression of TEs. To test this hypothesis, we combined the *h2a.w.6*, *h2a.w.7*, and *cmt3-11* null mutant alleles. This combination led to male and female gamete abortion (Figures S4B and S4C), and we were unable to obtain any triple homozygous plants out of 704 progeny segregating from the self-fertilized triple heterozygous mutant, indicating that CMT3 and H2A.W pathways are synergistically required for viability. CMT3 methylates heterochromatic DNA by binding to H3K9me2 (Du et al., 2012), and consistently, CHG methylation is reduced in *kyp* mutants (Jackson et al., 2002; Stroud et al., 2013). Accordingly, the synergistic action of H2A.W and KYP was also observed on expression of solo long terminal repeat

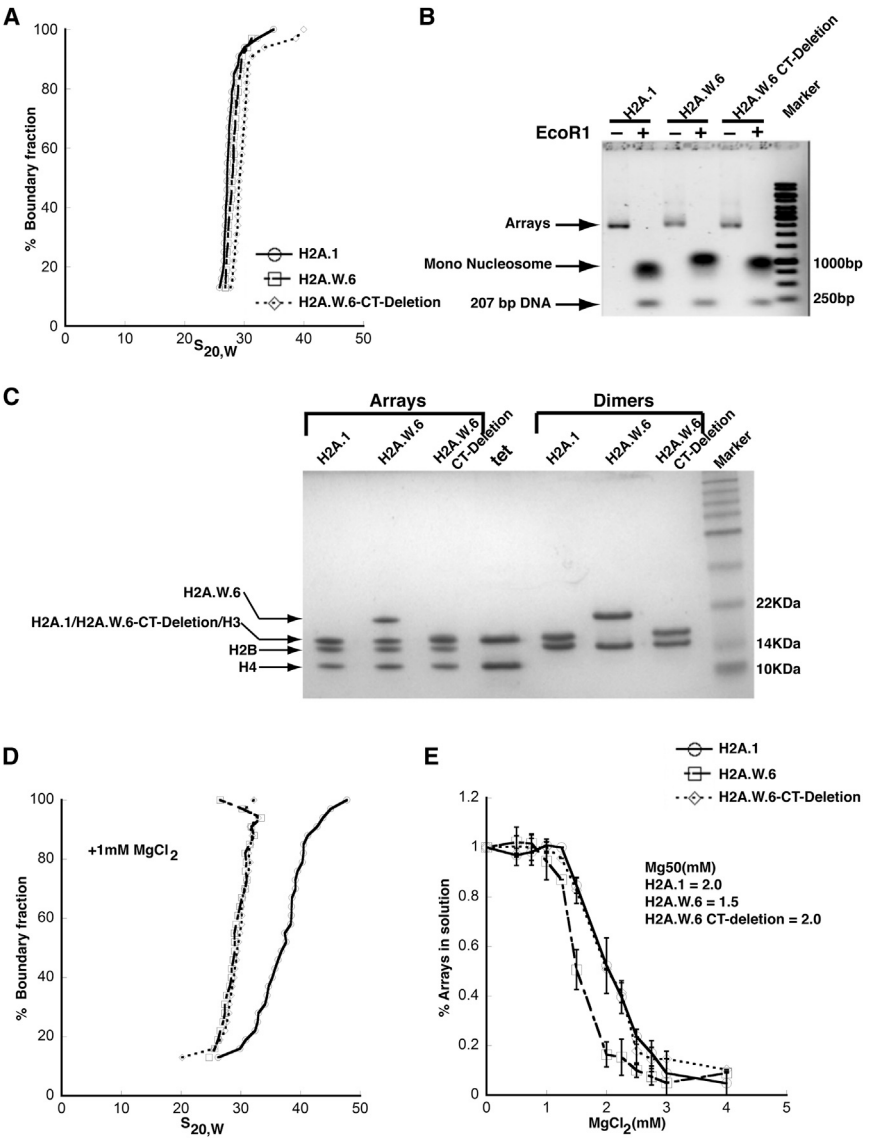

Figure 5. H2A.W Causes Chromatin Condensation through Chromatin Fiber-Fiber Interactions Promoted by its Conserved C-Terminal Tail In Vitro

(A) SV-AUC profile for 207-12 arrays assembled with H2A.1, H2A.W.6, and H2A.W.6-CT deletion indicates similar (and near-complete) saturation.

(B) EcoRI digestion of nucleosome arrays to assay the degree of saturation of each array. Each array exhibits similar amounts of free 207 bp DNA confirming similar saturation of the arrays.

(C) 1 to 2 μg of each array from (A) was run on a 15% SDS-PAGE to confirm equimolar distribution of histones. Tet indicates $(H3\text{-}H4)_2$ tetramer. Note that H2A.1 and H2A.W.6-CT deletion runs in the same position as H3 on the gel.

(D) The arrays were subjected to folding assay in the presence of 1 mM $MgCl_2$. The H2A.1-containing control arrays show moderate folding (midpoint S ~40S), whereas both H2A.W.6 and H2A.W.6-CT deletion containing arrays do not undergo folding under these conditions.

(E) Magnesium chloride-induced self-association assay showing that H2A.W.6 promotes inter-nucleosome array interactions. Arrays were incubated at the indicated concentrations of $MgCl_2$, and the concentration of Mg^{2+} at which 50% of the arrays have precipitated (Mg_{50}) is listed in the figure (inset). Error bars are derived from two independent measurements (two preparations of reconstituted arrays).

(LTR) TE and the gene *SDC*, which were both dramatically increased in the *h2a.w.6 h2a.w.7 kyp* triple mutant (Figure 4C). These data suggest that genetic pathways of H2A.W and CHG methylation interact to ensure heterochromatin integrity.

H2A.W Promotes Chromatin Condensation through Its Conserved C-Terminal Motif In Vitro

To further understand the potential mechanism of H2A.W in chromatin condensation, we tested whether H2A.W is able to cause condensation of nucleosome arrays in vitro. Chromatin condensation in vitro is composed of two independent structural transitions. Nucleosomes undergo short-range interactions with neighboring nucleosomes to form locally folded chromatin fibers. In addition, chromatin fibers self-associate to form supramolecular oligomers that share many of the properties of large-scale structure in condensed chromosomes. These two reversible structural transitions rely on different types of nucleosome-nucleosome interactions (Hansen, 2002) and can be studied in a model system by analyzing the magnesium-dependent solution-state properties of defined 12-mer nucleosomal arrays in vitro. To understand the mechanism of H2A.W in chromatin condensation in vitro, we tested whether H2A.W affects self-association or folding. We assembled nucleosome arrays with *Arabidopsis* H2A.1, H2A.W.6, or a truncated version of H2A.W.6 (H2A.W-CT) that lacks the C-terminal tail containing the SPKK motif (Figure 5). Because folding and self-association depend on the number of nucleosomes per array, the three types of arrays were closely matched for nucleosome saturation. We ensured that all arrays contain on average 11 to 12 nucleosomes per DNA molecule, i.e., every nucleosome positioning sequence repeat is occupied (Figures 5A and 5B). We also verified equimolar distribution of all histone components by SDS-PAGE (Figure 5C). We then determined the extent of self-association as a function of salt concentration and found that H2A.W.6 arrays engaged in oligomerization at significantly lower $MgCl_2$ concentrations than H2A.1 or H2A.W.6-CT (Figure 5E). This suggests that H2A.W.6 promotes long-range nucleosome-nucleosome interactions in chromosomes and that the C-terminal tail of H2A.W.6 contributes to this behavior. Intriguingly, both arrays with H2A.W.6 and H2A.W.6-CT exhibited no sign of folding at 1 mM $MgCl_2$, whereas arrays with canonical H2A.1

behave like other nucleosomal arrays and were moderately folded under these conditions (Figure 5D). Altogether, this suggests that H2A.W is able to enhance large-scale chromatin condensation by promoting long-range chromatin fiber-to-fiber interactions through its conserved C-terminal tail but is deficient in the short-range interactions that form the 30 nm fiber, suggesting a role in promoting highly condensed heterochromatin in vivo.

H2A.W Promotes Chromatin Condensation In Vivo

Because there was a gain of DNA methylation upon loss of H2A.W in *h2a.w* triple mutants (Figure 4A), it was difficult to address directly whether H2A.W is sufficient to promote heterochromatin condensation in somatic cells. However, we observed that none of the genes encoding H2A.W were expressed in the central cell, one of the two female gametes of flowering plants (Figures S5A–S5C). The absence of H2A.W in this cell type correlated with the complete absence of condensed heterochromatic domains as indicated by the uniform distribution of H2A.X.5-RFP (Figure 6A), which marks equally heterochromatin and euchromatin in somatic cells (Figures 1A–1D). In order to test whether the lack of H2A.W was responsible for the absence of condensed heterochromatin in the central cell nucleus, we ectopically expressed H2A.W.6 using the promoter of *FWA*, which is specifically active in the central cell and the endosperm (Kinoshita et al., 2004). The chromatin of the central cell expressing *pFWA-H2A.W.6-RFP* showed domains of varying intensity with distinct zones of higher condensation (Figure 6B). We could distinguish two types of organization. A minor group of nuclei showed one or two strong patches of dense chromatin. The most representative class of central cell nuclei showed several patches of dense chromatin assembled in the periphery of the nucleus (Figure 6B), contrasting with the uniform WT pattern of H2A.X-RFP that marks both euchromatin and heterochromatin (Figure 6A). To test whether the assembled condensed domains are heterochromatic, we immunostained whole ovules against H2A.X to report the general chromatin organization and against H3K9me2 to mark heterochromatin. We also used the POLYDACTYL ZINC FINGER (PZF)-GFP that binds to centromeric 180 bp repeats in somatic cells (Lindhout et al., 2007). In the WT, chromocenters marked by chromatin condensation and H3K9me2 were clearly observed in the egg cell nucleus (Figures 6C), whereas the central cell chromatin organization was more diffuse with elongated patches of H3K9me2 lining the periphery of the nucleus (Figure 6C). In contrast, central cells expressing H2A.W.6-RFP clearly showed dense chromatin domains marked by H3K9me2, indicating that these domains are heterochromatic. In addition, within these domains, we detected a single dot of centromeric marker PZF-GFP (Figure 6D, bottom), indicating that condensed chromatin domains caused by ectopic H2A.W are indeed pericentromeric heterochromatin foci. The absence of visible dots of PZF-GFP in WT central cell nuclei (Figure 6D, WT) was likely explained by the decondensed status of the pericentromeric and centromeric domains in the central cell and the absence of the cenH3 assembly reported previously (Ingouff et al., 2010). These observations indicate that H2A.W is sufficient to cause heterochromatin condensation in vivo.

DISCUSSION

Comprehensive genomic profiling showed that each H2A variant is characterized by a specific profile. In contrast to H2A, H2A.Z, and H2A.W, the distribution of H2A.X is relatively ubiquitous, which is in keeping with the idea that H2A.X is involved in DNA repair (Downs et al., 2007; Soria et al., 2012). H2A uniformly marks gene bodies similar to that described for H3.1 (Stroud et al., 2012; Wollmann et al., 2012). Transcription of both H3.1 and H2A is highly coupled with S phase (Talbert et al., 2012), suggesting that H2A and H3.1 are likely subject to common dynamics related to the loading of new nucleosomes over replicated DNA. However, unlike H3.1, H2A enrichment over gene bodies positively correlates with transcription with a gradual replacement by H2A.Z in genes expressed at low levels, suggesting that transcription is coupled to an exchange between H2A and H2A.Z over gene bodies. We confirmed that, in highly expressed genes, H2A.Z enrichment is confined to the 5′ end of the gene bodies, similar to that described in yeast, *Drosophila*, and human (Zilberman et al., 2008). This enrichment appears to be a mirror image of H3.3 distribution, confined to the 3′ end of gene bodies (Stroud et al., 2012; Wollmann et al., 2012). Hence, the boundaries of gene bodies appear to be defined by differential enrichment of H2A, H2A.Z, and H3.3 variants. In sharp contrast to euchromatin, heterochromatin is depleted of H2A and H2A.Z and is occupied by H2A.W, suggesting that H2A variants restrict the deposition of each other over larger genomic domains defining euchromatin and heterochromatin. Therefore, combinatorial localizations of H2A and H3 variants define the main genomic features in *Arabidopsis*.

We show that H2A.W recruitment to chromatin is independent of the pathways that deposit heterochromatic marks H3K9me2 and DNA methylation. However, H2A.W acts together with these pathways to maintain heterochromatin condensation into higher-order domains and to silence TEs. The lethal genetic interaction observed in our study suggests that H2A.W and H3K9me2/CHG methylation are absolutely essential for plant life. The lethality observed in mutants deficient for both pathways likely results from a lack of heterochromatin integrity, which could impact cell division. In response to H2A.W depletion, we also observe a crosstalk between these pathways as both CMT3 expression and CHG methylation increase in heterochromatin.

In vitro micrococcal nuclease digestion data showed that nucleosomes containing H2A.W protect a longer stretch of DNA (162 bp) than nucleosomes containing H2A (146 bp) (Lindsey et al., 1991), suggesting that H2A.W prevents accessibility to DNA. Consistently, we find that H2A.W represses TE expression in synergistic action with H3K9me2. The acidic patch present in the histone core region of H2A affects the folding ability of nucleosome arrays (Kalashnikova et al., 2013). For example, euchromatic H2A.Z shows higher chromatin folding than H2A as a consequence of its extended acidic patch (Fan et al., 2004). The acidic patch in H2A.W and canonical H2A are identical, and H2A.W shows a lower folding capacity than H2A, suggesting that other domains of H2A participate in chromatin folding. Our results show that H2A.W promotes chromatin condensation through long-range fiber-to-fiber interactions in vitro. These

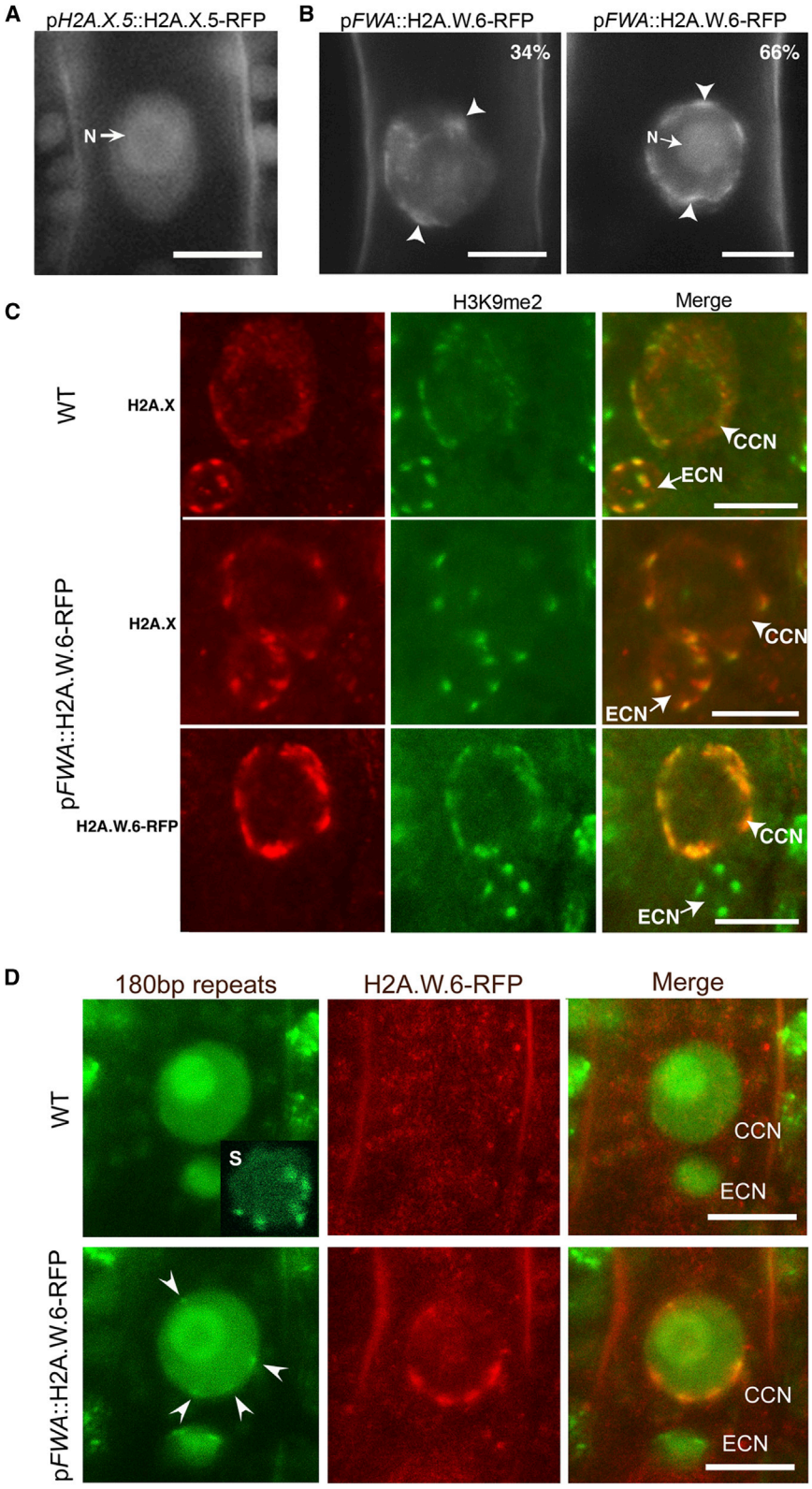

Figure 6. H2A.W Is Sufficient to Cause Chromatin Condensation In Vivo

(A) Uniform pattern of p*H2A.X.5*-H2A.X.5-RFP expressed in the central cell nucleus indicating the absence of defined chromocenters. N points the nucleolus.

(B) Impact of ectopic expression of *H2A.W.6-RFP* in the central cell nucleus (CCN). We observe mild or severe chromatin condensation (arrowheads), and the proportion of each type of nuclei is indicated in the top right of each image. N points the nucleolus.

(C) Impact of ectopic expression of *H2A.W.6-RFP* in the CCN on H2A.X and H3K9me2 immunolocalization. Top: the egg cell nucleus (ECN) shows well-defined chromocenters reported by H2A.X condensation and marked with H3K9me2 and serves as a reference point for comparison with the CCN. Middle: ectopic expression of H2A.W.6 in the CCN causes condensation of chromatin domains reported by H2A.X. Bottom: these domains are marked with H3K9me2 (lower panel).

(D) A CCN-expressing PZF-GFP that recognizes the centromeric 180 bp repeats. Top: in the WT, PZF-GFP marks condensed centromeres in somatic cells (S, insert, a nucleus from root cells) but does not mark any condensed structure in the CCN. Bottom: in a central cell expressing *pFWA::H2A.W.6-RFP*, arrowheads point the position of condensed chromatin domains, which contain a dot of PZF-GFP marking the centromeric location. Scale bars in confocal sections represent 5 μm.

See also Figure S5.

data are supported by the contrasting impacts of loss or gain of function of H2A.W in vivo on heterochromatin organization. We propose that H2A.W is necessary and sufficient to organize heterochromatin into higher-order functional domains such as chromocenters, which are essential for kinetochore assembly and mitosis (Bian and Belmont, 2012; Luger et al., 2012).

H2A.W-specific chromatin condensation properties rely on the extended C-terminal domain that contains the conserved SPKK motif. This is consistent with previous in vitro studies of the function of the SPKK motif in other histone variants (Khadake and Rao, 1997). The SPKK motif binds preferentially to the minor groove of DNA at A/T rich sites (Churchill and Suzuki, 1989), which are generally enriched in satellite repeats of heterochromatin (Brutlag, 1980). During evolution, the SPKK motif not only became associated with H2A.W in seed plants but was also recruited to other histones, which are associated with condensed chromatin, the linker H1 in most eukaryotes, and the sea urchin testis-specific H2B (Suzuki, 1989; Buttinelli et al., 1999; Poccia and Green, 1992). Motifs similar to SPKK are also present in the linker region of the vertebrate-specific macroH2A that separates the core histone domain from the C-terminal macrodomain (Figure S6). MacroH2A is highly enriched on the X chromosome and is linked to transcriptional repression (Costanzi and Pehrson, 1998; Gamble et al., 2010; Gaspar-Maia et al., 2013). In vitro, the linker region of macroH2A causes chromatin condensation (Muthurajan et al., 2011), and macroH2A devoid of the macrodomain stabilizes nucleosomes (Chakravarthy et al., 2012). However, how macroH2A affects chromatin architecture in vivo remains unclear. The similarity between H2A.W and macroH2A devoid of its macrodomain suggests that the properties of H2A.W described in this study may reveal conserved aspects of histone variant functions that may not only aid in our understanding of plant heterochromatin but also shed light on mechanisms controlling higher-order heterochromatin condensation in other eukaryotes.

EXPERIMENTAL PROCEDURES

Plant Material and Growth Conditions

All mutants are in Columbia-0 (Col) ecotype. *h2a.w.6* (SALK_024544.32), *h2a.w.7* (GK_149G05), and *h2a.w.12* (SAIL_667) T-DNA lines were obtained from ABRC at Ohio State University and NASC at The University of Nottingham, respectively. *drm2-2* (SALK_150863.37.35), *cmt3-11* (SALK_148381), *kyp-6 (*SALK_041474), *suvh4,5,6* triple mutant (SALK_041474, Gabi_263C05, SAIL_1244_F04), *cmt3-11* (SALK_148381), *drm2-2* (SALK_150863), *met1-3*, and the EMS-induced SNP in *ddm1-2*. *met1-3*, *ddm1-2*, and *kyp suvh5 suvh6* were previously described (Johnson et al., 2008; Saze et al., 2003; Vongs et al., 1993). The 180 bp repeat reporter PDZ-GFP was a kind gift from Prof. B. van der Zaal. *h2a.w.6* and *h2a.w.7* T-DNA insertions were confirmed by PCR-based genotyping. Primer sequences are described in Table S1. *Arabidopsis* plants were grown under long day conditions—i.e., 16 hr light and 8 hr dark.

H2A Variants ChIP-Seq Analyses

ChIP was performed as previously described (Wollmann et al., 2012) with few modifications. Two grams of seedlings were ground in liquid nitrogen and fixed in 1% formaldehyde. Sonicated chromatin was incubated overnight with anti-H2A, anti-H2A.X, anti-H2A.W.6, anti-H2A.Z.9, and anti-H3 (ab1791, Abcam) antibodies or IgG (ab46540-1, Abcam). Immunoprecipitated DNA was treated with RNase A (Fermentas) and purified with the QIAquick purification kit (QIAGEN). ChIP-seq libraries were generated as per manufacturer's instructions (Illumina). Libraries were sequenced on a HiSeq2000 (Illumina). Reads were mapped to the TAIR8 genome, and analysis was performed as previously described (Stroud et al., 2012).

DNA Methylation Analyses

For genome-wide bisulfite sequencing (BS-seq), plants were grown under continuous light, and samples were collected from 3-week-old plants. Genomic DNA was extracted using Plant DNeasy Mini kit (QIAGEN). BS-seq libraries were generated, sequenced, and analyzed exactly as previously described (Stroud et al., 2013), except that reads were mapped to the TAIR8 genome.

Nucleosome Array Assembly

Nucleosomal arrays were reconstituted onto a DNA fragment that comprises 12 repeats of 207 base pairs "601" positioning sequence (Lowary and Widom, 1998). A two-step reconstitution method was applied to assemble nucleosome arrays (Muthurajan et al., 2011). First, different amounts of $(H3\text{-}H4)_2$ tetramers were titrated to DNA. The tetrasomes were reconstituted by step dialysis (4–6 hr each step) starting from 1 M NaCl to 0.75 M NaCl and finally 2.5 mM NaCl (in a buffer containing 10 mM Tris [pH 7.5] and 0.25 mM EDTA). The best ratio between H3-H4 and DNA for tetrasome formation was determined by sedimentation velocity AUC. Once the $S_{20,w}$ midpoint of reconstitution reached around 19S, the ratio of tetramer to DNA was fixed for the next step. Varying amounts of variant H2A-H2B dimers were added to the optimized the ratio of tetramer to DNA. The saturation levels of arrays were determined by sedimentation velocity AUC (SV-AUC). To reach a $S_{20,w}$ of 29S (characteristic of a fully saturated array), the ratio of dimer to tetrasome was around 2.0. EcoRI digestion also was be used to monitor the saturation status of nucleosome arrays as described previously (Muthurajan et al., 2011).

Self-Association Assay

Nucleosomal arrays (the equivalent of ~1 μg DNA) were combined with various concentrations of $MgCl_2$ (from 0 to 5 mM). The mixtures were incubated at room temperature for 5 min and then spun at 14,000 g for 10 min. The percentage of arrays remaining in the supernatant was determined at 259 nm and was plotted against the concentration of $MgCl_2$.

Folding Assay by Sedimentation Velocity

Nucleosome arrays containing ~10 μg DNA were treated with 1 mM $MgCl_2$. SV-AUC was applied to monitor the impact of $MgCl_2$ on array folding. Sedimentation velocity experiments were done in a Beckman XL-A or XL-I ultracentrifuge at 20,000 rpm and 20°C. The absorbance at 259 nm was scanned continuously with a redial increment of 0.003 cm. All results were processed and analyzed by UltraScanIII. By the improved van Holde-Weischet method in UltraScanIII, the diffusion-corrected integral distribution (G(s)) of sedimentation coefficients over the entire boundaries was analyzed and plotted.

ACCESSION NUMBERS

The sequencing data are deposited at Gene Expression Omnibus (GEO) with the accession number GSE50942.

SUPPLEMENTAL INFORMATION

Supplemental Information includes Extended Experimental Procedures, six figures, and one table and can be found with this article online at http://dx.doi.org/10.1016/j.cell.2014.06.006.

AUTHOR CONTRIBUTIONS

K.Z., U.M.M., and K.L. performed experiments reported in Figures 5 and S5; S.F. and X.Z. performed the first series of ChIP-seq for H2A.W.6; S.F. performed genome-wide bisulfite sequencing; H.S. performed the RNA-seq and all bioinformatic analyses; S.H. participated in H2A variants ChIP; S.H., T.K., and F.B. produced the data shown in Figures 6 and S6; X.N. performed preliminary transcriptome analyses; M.G. provided Figure S2H; and R.Y. performed

all other experiments and analyses. F.B. conceived the initial project, which was developed with the help of a fruitful collaboration with the S.E.J. lab. R.Y., F.B., and S.E.J. wrote the manuscript with inputs from all other authors.

ACKNOWLEDGMENTS

R.Y., S.H., X.N., and F.B. were funded by Temasek Life Sciences Laboratory. Sequencing was performed at the UCLA BSCRC BioSequencing Core facility. We thank Meredith Calvert for help with imaging and Mahnaz Akhavan for Illumina sequencing. We thank Dr. Maruyama for his comments and support with the graphical abstract. H.S. was supported by a Dissertation Year Fellowship from UCLA. X.Z. is a research fellow of Ruth L. Kirschstein National Research Service Award (F32GM096483-01). S.F. is a Special Fellow of the Leukemia & Lymphoma Society. Work in the Jacobsen lab was supported by NSF grant 1121245. K.L., U.M., and K.Z. are supported by NIH-GM067777. M.G. is supported by EMBO ALTF 986-2011 and HHMI. S.E.J. and K.L. are Investigators of the Howard Hughes Medical Institute.

Received: November 29, 2013
Revised: March 14, 2014
Accepted: May 14, 2014
Published: July 3, 2014

REFERENCES

Aceituno, F.F., Moseyko, N., Rhee, S.Y., and Gutiérrez, R.A. (2008). The rules of gene expression in plants: organ identity and gene body methylation are key factors for regulation of gene expression in Arabidopsis thaliana. BMC Genomics *9*, 438.

Bernatavichute, Y.V., Zhang, X., Cokus, S., Pellegrini, M., and Jacobsen, S.E. (2008). Genome-wide association of histone H3 lysine nine methylation with CHG DNA methylation in Arabidopsis thaliana. PLoS ONE *3*, e3156.

Bian, Q., and Belmont, A.S. (2012). Revisiting higher-order and large-scale chromatin organization. Curr. Opin. Cell Biol. *24*, 359–366.

Bönisch, C., and Hake, S.B. (2012). Histone H2A variants in nucleosomes and chromatin: more or less stable? Nucleic Acids Res. *40*, 10719–10741.

Brutlag, D.L. (1980). Molecular arrangement and evolution of heterochromatic DNA. Annu. Rev. Genet. *14*, 121–144.

Buttinelli, M., Panetta, G., Rhodes, D., and Travers, A. (1999). The role of histone H1 in chromatin condensation and transcriptional repression. Genetica *106*, 117–124.

Chakravarthy, S., Patel, A., and Bowman, G.D. (2012). The basic linker of macroH2A stabilizes DNA at the entry/exit site of the nucleosome. Nucleic Acids Res. *40*, 8285–8295.

Churchill, M.E.A., and Suzuki, M. (1989). 'SPKK' motifs prefer to bind to DNA at A/T-rich sites. EMBO J. *8*, 4189–4195.

Coleman-Derr, D., and Zilberman, D. (2012). Deposition of histone variant H2A.Z within gene bodies regulates responsive genes. PLoS Genet. *8*, e1002988.

Costanzi, C., and Pehrson, J.R. (1998). Histone macroH2A1 is concentrated in the inactive X chromosome of female mammals. Nature *393*, 599–601.

De Rop, V., Padeganeh, A., and Maddox, P.S. (2012). CENP-A: the key player behind centromere identity, propagation, and kinetochore assembly. Chromosoma *121*, 527–538.

Downs, J.A., Nussenzweig, M.C., and Nussenzweig, A. (2007). Chromatin dynamics and the preservation of genetic information. Nature *447*, 951–958.

Du, J., Zhong, X., Bernatavichute, Y.V., Stroud, H., Feng, S., Caro, E., Vashisht, A.A., Terragni, J., Chin, H.G., Tu, A., et al. (2012). Dual binding of chromomethylase domains to H3K9me2-containing nucleosomes directs DNA methylation in plants. Cell *151*, 167–180.

Fan, J.Y., Rangasamy, D., Luger, K., and Tremethick, D.J. (2004). H2A.Z alters the nucleosome surface to promote HP1α-mediated chromatin fiber folding. Mol. Cell *16*, 655–661.

Fang, Y., and Spector, D.L. (2005). Centromere positioning and dynamics in living Arabidopsis plants. Mol. Biol. Cell *16*, 5710–5718.

Filipescu, D., Szenker, E., and Almouzni, G. (2013). Developmental roles of histone H3 variants and their chaperones. Trends Genet. *29*, 630–640.

Finnegan, E.J., and Dennis, E.S. (1993). Isolation and identification by sequence homology of a putative cytosine methyltransferase from Arabidopsis thaliana. Nucleic Acids Res. *21*, 2383–2388.

Fransz, P., De Jong, J.H., Lysak, M., Castiglione, M.R., and Schubert, I. (2002). Interphase chromosomes in Arabidopsis are organized as well defined chromocenters from which euchromatin loops emanate. Proc. Natl. Acad. Sci. USA *99*, 14584–14589.

Gamble, M.J., Frizzell, K.M., Yang, C., Krishnakumar, R., and Kraus, W.L. (2010). The histone variant macroH2A1 marks repressed autosomal chromatin, but protects a subset of its target genes from silencing. Genes Dev. *24*, 21–32.

Gaspar-Maia, A., Qadeer, Z.A., Hasson, D., Ratnakumar, K., Leu, N.A., Leroy, G., Liu, S., Costanzi, C., Valle-Garcia, D., Schaniel, C., et al. (2013). MacroH2A histone variants act as a barrier upon reprogramming towards pluripotency. Nat. Commun. *4*, 1565.

Goldberg, A.D., Banaszynski, L.A., Noh, K.-M., Lewis, P.W., Elsaesser, S.J., Stadler, S., Dewell, S., Law, M., Guo, X., Li, X., et al. (2010). Distinct factors control histone variant H3.3 localization at specific genomic regions. Cell *140*, 678–691.

Guillemette, B., Bataille, A.R., Gévry, N., Adam, M., Blanchette, M., Robert, F., and Gaudreau, L. (2005). Variant histone H2A.Z is globally localized to the promoters of inactive yeast genes and regulates nucleosome positioning. PLoS Biol. *3*, e384.

Haag, J.R., and Pikaard, C.S. (2011). Multisubunit RNA polymerases IV and V: purveyors of non-coding RNA for plant gene silencing. Nat. Rev. Mol. Cell Biol. *12*, 483–492.

Hansen, J.C. (2002). Conformational dynamics of the chromatin fiber in solution: determinants, mechanisms, and functions. Annu. Rev. Biophys. Biomol. Struct. *31*, 361–392.

Ingouff, M., Rademacher, S., Holec, S., Soljić, L., Xin, N., Readshaw, A., Foo, S.H., Lahouze, B., Sprunck, S., and Berger, F. (2010). Zygotic resetting of the HISTONE 3 variant repertoire participates in epigenetic reprogramming in Arabidopsis. Curr. Biol. *20*, 2137–2143.

Jackson, J.P., Lindroth, A.M., Cao, X., and Jacobsen, S.E. (2002). Control of CpNpG DNA methylation by the KRYPTONITE histone H3 methyltransferase. Nature *416*, 556–560.

Jeddeloh, J.A., Stokes, T.L., and Richards, E.J. (1999). Maintenance of genomic methylation requires a SWI2/SNF2-like protein. Nat. Genet. *22*, 94–97.

Jenuwein, T., and Allis, C.D. (2001). Translating the histone code. Science *293*, 1074–1080.

Kalashnikova, A.A., Porter-Goff, M.E., Muthurajan, U.M., Luger, K., and Hansen, J.C. (2013). The role of the nucleosome acidic patch in modulating higher order chromatin structure. J. R. Soc. Interface *10*, 20121022.

Khadake, J.R., and Rao, M.R.S. (1997). Condensation of DNA and chromatin by an SPKK-containing octapeptide repeat motif present in the C-terminus of histone H1. Biochemistry *36*, 1041–1051.

Kinoshita, T., Miura, A., Choi, Y., Kinoshita, Y., Cao, X., Jacobsen, S.E., Fischer, R.L., and Kakutani, T. (2004). One-way control of FWA imprinting in Arabidopsis endosperm by DNA methylation. Science *303*, 521–523.

Law, J.A., and Jacobsen, S.E. (2010). Establishing, maintaining and modifying DNA methylation patterns in plants and animals. Nat. Rev. Genet. *11*, 204–220.

Li, B., Pattenden, S.G., Lee, D., Gutiérrez, J., Chen, J., Seidel, C., Gerton, J., and Workman, J.L. (2005). Preferential occupancy of histone variant H2AZ at inactive promoters influences local histone modifications and chromatin remodeling. Proc. Natl. Acad. Sci. USA *102*, 18385–18390.

Lindhout, B.I., Fransz, P., Tessadori, F., Meckel, T., Hooykaas, P.J., and van der Zaal, B.J. (2007). Live cell imaging of repetitive DNA sequences via GFP-tagged polydactyl zinc finger proteins. Nucleic Acids Res. *35*, e107.

Lindroth, A.M., Cao, X., Jackson, J.P., Zilberman, D., McCallum, C.M., Henikoff, S., and Jacobsen, S.E. (2001). Requirement of CHROMOMETHYLASE3 for maintenance of CpXpG methylation. Science *292*, 2077–2080.

Lindsey, G.G., Orgeig, S., Thompson, P., Davies, N., and Maeder, D.L. (1991). Extended C-terminal tail of wheat histone H2A interacts with DNA of the "linker" region. J. Mol. Biol. *218*, 805–813.

Lowary, P.T., and Widom, J. (1998). New DNA sequence rules for high affinity binding to histone octamer and sequence-directed nucleosome positioning. J. Mol. Biol. *276*, 19–42.

Loyola, A., and Almouzni, G. (2007). Marking histone H3 variants: how, when and why? Trends Biochem. Sci. *32*, 425–433.

Luger, K., Mäder, A.W., Richmond, R.K., Sargent, D.F., and Richmond, T.J. (1997). Crystal structure of the nucleosome core particle at 2.8 A resolution. Nature *389*, 251–260.

Luger, K., Dechassa, M.L., and Tremethick, D.J. (2012). New insights into nucleosome and chromatin structure: an ordered state or a disordered affair? Nat. Rev. Mol. Cell Biol. *13*, 436–447.

Lysak, M., Fransz, P., and Schubert, I. (2006). Cytogenetic analyses of Arabidopsis. Methods Mol. Biol. *323*, 173–86.

Malagnac, F., Bartee, L., and Bender, J. (2002). An Arabidopsis SET domain protein required for maintenance but not establishment of DNA methylation. EMBO J. *21*, 6842–6852.

Meneghini, M.D., Wu, M., and Madhani, H.D. (2003). Conserved histone variant H2A.Z protects euchromatin from the ectopic spread of silent heterochromatin. Cell *112*, 725–736.

Millar, C.B. (2013). Organizing the genome with H2A histone variants. Biochem. J. *449*, 567–579.

Mito, Y., Henikoff, J.G., and Henikoff, S. (2005). Genome-scale profiling of histone H3.3 replacement patterns. Nat. Genet. *37*, 1090–1097.

Muthurajan, U.M., McBryant, S.J., Lu, X., Hansen, J.C., and Luger, K. (2011). The linker region of macroH2A promotes self-association of nucleosomal arrays. J. Biol. Chem. *286*, 23852–23864.

Poccia, D.L., and Green, G.R. (1992). Packaging and unpackaging the sea urchin sperm genome. Trends Biochem. Sci. *17*, 223–227.

Raisner, R.M., Hartley, P.D., Meneghini, M.D., Bao, M.Z., Liu, C.L., Schreiber, S.L., Rando, O.J., and Madhani, H.D. (2005). Histone variant H2A.Z marks the 5′ ends of both active and inactive genes in euchromatin. Cell *123*, 233–248.

Reinders, J., Wulff, B.B., Mirouze, M., Marí-Ordóñez, A., Dapp, M., Rozhon, W., Bucher, E., Theiler, G., and Paszkowski, J. (2009). Compromised stability of DNA methylation and transposon immobilization in mosaic Arabidopsis epigenomes. Genes Dev. *23*, 939–950.

Soria, G., Polo, S.E., and Almouzni, G. (2012). Prime, repair, restore: the active role of chromatin in the DNA damage response. Mol. Cell *46*, 722–734.

Stroud, H., Otero, S., Desvoyes, B., Ramírez-Parra, E., Jacobsen, S.E., and Gutierrez, C. (2012). Genome-wide analysis of histone H3.1 and H3.3 variants in Arabidopsis thaliana. Proc. Natl. Acad. Sci. USA *109*, 5370–5375.

Stroud, H., Greenberg, M.V.C., Feng, S., Bernatavichute, Y.V., and Jacobsen, S.E. (2013). Comprehensive analysis of silencing mutants reveals complex regulation of the Arabidopsis methylome. Cell *152*, 352–364.

Stroud, H., Do, T., Du, J., Zhong, X., Feng, S., Johnson, L., Patel, D.J., and Jacobsen, S.E. (2014). Non-CG methylation patterns shape the epigenetic landscape in Arabidopsis. Nat. Struct. Mol. Biol. *21*, 64–72.

Suzuki, M. (1989). SPKK, a new nucleic acid-binding unit of protein found in histone. EMBO J. *8*, 797–804.

Szenker, E., Ray-Gallet, D., and Almouzni, G. (2011). The double face of the histone variant H3.3. Cell Res. *21*, 421–434.

Talbert, P.B., and Henikoff, S. (2010). Histone variants—ancient wrap artists of the epigenome. Nat. Rev. Mol. Cell Biol. *11*, 264–275.

Talbert, P.B., Masuelli, R., Tyagi, A.P., Comai, L., and Henikoff, S. (2002). Centromeric localization and adaptive evolution of an Arabidopsis histone H3 variant. Plant Cell *14*, 1053–1066.

Talbert, P., Bayes, J., and Henikoff, S. (2008). Evolution of centromeres and kinetochores: A two-part fugue. In The Kinetochore: From Molecular Discoveries to Cancer Therapy, P. De Wulf and W.C. Earnshaw, eds. (New York: Springer), pp. 193–230.

Talbert, P.B., Ahmad, K., Almouzni, G., Ausió, J., Berger, F., Bhalla, P.L., Bonner, W.M., Cande, W.Z., Chadwick, B.P., Chan, S.W., et al. (2012). A unified phylogeny-based nomenclature for histone variants. Epigenetics Chromatin *5*, 7.

Vaillant, I., Tutois, S., Jasencakova, Z., Douet, J., Schubert, I., and Tourmente, S. (2008). Hypomethylation and hypermethylation of the tandem repetitive 5S rRNA genes in Arabidopsis. Plant J. *54*, 299–309.

Vongs, A., Kakutani, T., Martienssen, R.A., and Richards, E.J. (1993). Arabidopsis thaliana DNA methylation mutants. Science *260*, 1926–1928.

Wollmann, H., Holec, S., Alden, K., Clarke, N.D., Jacques, P.-E., and Berger, F. (2012). Dynamic deposition of histone variant H3.3 accompanies developmental remodeling of the *Arabidopsis* transcriptome. PLoS Genet. *8*, e1002658.

Wong, L.H., Ren, H., Williams, E., McGhie, J., Ahn, S., Sim, M., Tam, A., Earle, E., Anderson, M.A., Mann, J., and Choo, K.H. (2009). Histone H3.3 incorporation provides a unique and functionally essential telomeric chromatin in embryonic stem cells. Genome Res. *19*, 404–414.

Zemach, A., Kim, M.Y., Hsieh, P.-H., Coleman-Derr, D., Eshed-Williams, L., Thao, K., Harmer, S.L., and Zilberman, D. (2013). The Arabidopsis nucleosome remodeler DDM1 allows DNA methyltransferases to access H1-containing heterochromatin. Cell *153*, 193–205.

Zilberman, D., Coleman-Derr, D., Ballinger, T., and Henikoff, S. (2008). Histone H2A.Z and DNA methylation are mutually antagonistic chromatin marks. Nature *456*, 125–129.